Effective Use of Magnetization Data in the Design of Electric Machines with Overfluxed Regions

Dantam K. Rao[1], and Vladimir Kuptsov[2]

[1]MagWeb USA, Schenectady, 12309 USA
[2]Magnitogorsk Iron and Steel Works, Magnitogorsk City, RUSSIA

Electric machines often have overfluxed regions that carry large magnetic fields that are beyond the maximum value for which magnetization data is available. These fields are close to magnetic saturation, so extrapolation to saturation is required to accurately map the overfluxed regions. But the extrapolation methods used in most magnetic field software do not consider the physics of saturation, so they are known to cause significant errors.

The Simultaneous Exponential Extrapolation procedure (SEE) presented herein incorporates the physics of saturation. It essentially converts the extrapolation problem into an interpolation problem by forcing it to pass through a point close to saturation, thereby minimizing errors. This paper also discusses potential hidden noise in the measured data that can cause numerical instability. It outlines a graphical procedure to remove such hidden noise to facilitate faster convergence. These extrapolation to saturation and the hidden-noise elimination procedures facilitate more accurate mapping of the overfluxed regions and allow better assessment of their impact of such regions on the performance of electric machines.

***Index Terms*— Electromagnetic Fields, Extrapolation to Saturation, Magnetic Materials, Overfluxed regions, Saturation Induction.**

I. Introduction

TORUE-DENSE electric machines are often designed to carry magnetic flux density about of about 1.5 T at rated conditions. But, under severe operating conditions, some regions, termed overfluxed regions herein, can carry significantly higher flux densities that may be close to saturation. Because they carry flux at higher densities, overfluxed regions run hotter. Because they are close to saturation, they leak flux. A machine with large overfluxed regions can leak relatively large flux which induce large eddy currents in the neighboring metallic parts (such as coils, clamping plates etc.), causing them also to run hotter. The joint damage can cause a machine to fail, reduce its life, or restrict the operational envelope [19] [26] [32] [39]. The severity of such adverse impact of the overfluxed regions depends on their flux density, size and location. So, accurate mapping of the overfluxed regions, and controlling their adverse effects, is a critical part of design of electric machines.

The flux density in the overfluxed regions is generally close to the saturation induction B_s of about 2 T. For example, induction motors can see ~ 3T in the rotor slots under locked rotor conditions [15], [30]. Large electric machines can see ~ 2.1 T in the core-end teeth under 0.95 leading power factor or underexcited conditions [31] [32]. Large transformers can see ~ 2.2 T in the core bolts during ferroresonance [58] [59] [14] [17]. HEV motors operating in deep saturation segment require substantially larger inverters [55]. So, generally the overfluxed regions carry local fields of more than 1.9 T, and they can adversely affect the performance of a machine.

Manuscript received 24 May 2014. Corresponding author: Dantam K. Rao (e-mail: rao@magweb.us).
Digital Object Identifier inserted by IEEE

The magnetization characteristic of electrical steels is usually measured in accordance with well-known international standards [48]. It is expressed as a single-valued B(H) curve where B denotes magnetic flux density in Tesla and H denotes the applied magnetic field intensity H in A/m. These tests are conducted by assembling cut steel strips into an Epstein frame and plotting a series of multi-valued B-H hysteresis loops of increasing intensity. A single-valued B(H) curve is then obtained by joining the tips of these escalating hysteresis loops [2]. A tabulated data of this B(H) curve, called B-H data, is inputted into commercial magnetic field software and is used in the design of an electric machine. But the maximum value of such measured B-H data rarely exceeds about 1.8 T as either the test standards restrict the test range to 1.8 T [48], the test frame overheats or the signals get distorted at fields higher than 1.8 T. Thus, the B-H data measured according to international standards is rarely available at levels above 1.9 T that are seen by the overfluxed regions [58] [59].

To accurately map the overfluxed regions, one therefore needs extrapolation of the measured B-H data beyond the measurement range [51- 56]. This problem, known as the extrapolation to saturation problem, requires significant engineering judgment on how best to extrapolate the steel properties beyond the measurement range. Ideally, such extrapolation should reflect the physical phenomenon of saturation of magnetic materials. But at present, most extrapolation procedures (used by most magnetic field software or manufacturing facilities) do not account for the phenomenon of saturation of magnetic materials. For example, they do not allow inputting of the saturation induction B_s of a specific steel. As a result, these methods can result in significant errors [14] [16] [53] [55].

So, in section II and III we introduce the requirements of saturation and discuss the prior art of extrapolation respectively. In section IV, we propose two procedures that incorporate the physics of saturation in the extrapolation process. These are Simultaneous Exponential Extrapolation (SEE) and Simultaneous Polynomial Extrapolation (SPE). They essentially convert the extrapolation problem into an interpolation problem by forcing the extrapolated curve to pass through a known point that is close to saturation, thereby ensuring it meets the saturation requirements. Comparison of these two procedures with other prior procedures indicates that SEE produces the least error.

Further, the measured B-H data can sometimes contain hidden noise that can cause numerical instabilities [34] [33] [35]. In section V, we propose a procedure to remove such hidden noise in the measured data. Such noise-free data is shown to increase the computational stability and result in faster convergence.

In summary, we propose a SEE procedure to extrapolate to saturation. We also propose a procedure to remove any hidden noise in the data that can affect the numerical stability. Both these procedures facilitate more accurate mapping of the overfluxed regions, thereby control their adverse impact on the performance of the machine. Thus, their usage can improve the effectiveness of using measured data in designing electric machines.

II. Extrapolation Requirements

Saturation of a magnetic material is best understood by expressing the magnetization curve B(H) as sum of a *Ferric Flux Density* J (aka magnetic polarization) and a *Vacuum Flux Density* $\mu_0 H$ [1] [2]. J denotes the flux density carried by the magnetic material alone; materials have a limited capacity to carry flux, so can get saturated. $\mu_0 H$ denotes the flux density carried by vacuum; such "free space" has unlimited capacity to carry flux, so can never get saturated. Saturation is best characterized by the *normalized slope* D(H) of the magnetization curve (aka slope, differential permeability). The two functions B(H) and D(H) with three parameters B, J, D needed to describe the saturation phenomenon are

$$B(H) = J + \mu_0 H \quad .... \quad .... \qquad (1)$$

$$D(H) \equiv \frac{1}{\mu_o}\frac{dB}{dH}$$

where $\mu_0 = 4\pi x10\text{-}7\ N/A^2$. A magnetic material is said to saturate when the dipole moments of all atoms in all crystals of all domains are fully aligned with H. Thus as H increases indefinitely, J(H) reaches an asymptotic limit, called *Saturation Induction* B_s (aka Saturation Polarization J_s, Saturation Magnetization) while the slope D(H) reaches an asymptotic limit of 1. Thus, the phenomenon of saturation is described by the asymptotic limits of B_s for ferric flux density J and 1 for the slope or differential permeability D :

$$\lim_{H \to \infty} \quad J(H) = B_s$$

$$\lim_{H \to \infty} \quad D(H) = 1 \quad \cdots \quad (2)$$

So the horizontal line $J(H) = B_s$ is asymptotic to the J(H) curve and the horizontal line D(H) = 1 is asymptotic to the D(H) curve. Thus, the requirements for extrapolation to saturation are: (1) J(H) must asymptotically reach the saturation induction B_s . (2) J(H) must always be *below* the asymptotic line $J(H) = B_s$. (3) The slope D(H) must asymptotically reach 1. (4) D(H) must always be *above* the asymptotic line D(H) = 1.

Fig. 1 illustrates magnetic characteristic of a typical non-grain oriented electrical steel. It shows as dots the last few measured B-H data points upto the last point B_n , plus the continuous extrapolation curves B(H), J(H) and D(H) that extend beyond the last point B_n . These continuous curves have two segments: (a) pre-saturation segment, where the slope D decays to about 10 nonlinearly, and (b) deep saturation segment, where the slope D decays from 1.5 to about 1 almost linearly. It also shows the asymptotic lines J = B_s and J = 1 that define the saturation. It indicates that the ferric flux density J(H) is always *less* than B_s while the slope D(H) is always *greater* than 1.

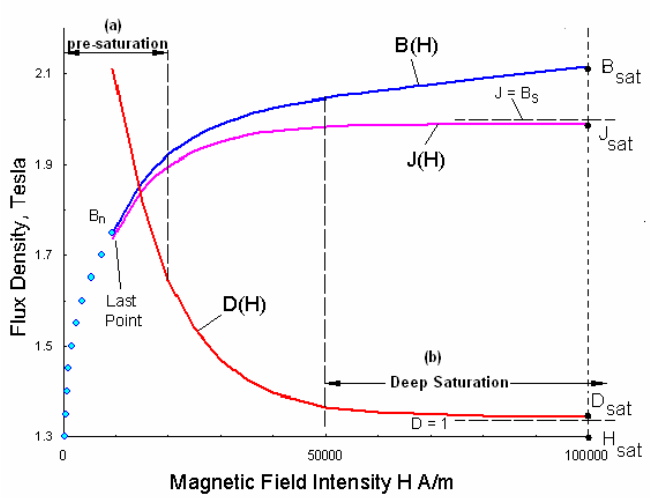

Fig. 1 Extrapolation to saturation requires the B(H) curve that is non-asymptotic plus the J (H) and D(H) curves that are asymptotic. A sat point, identified by subscript "sat", is one with J_{sat} very close to saturation induction B_s and the slope D_{sat} very close to 1. It is in the deep saturation regime and emulates the saturation of a magnetic material.

We define a point in the deep saturation segment, called "sat point" (H_{sat}, B_{sat}, J_{sat}, D_{sat}), identified by a subscript "sat". A sat point is that at which the ferric flux density J(H) is so close to B_s and the slope D(H) is so close to 1 that, for all practical purposes, it is synonymous to saturation. Because it is hard to measure the saturation induction B_s with an accuracy of less than 1% because of experimental scatter, a point at

which the slope D deviates at most by 1 % from the saturation slope of 1 (D_{sat} < 1.01) can be considered as a sat point. Beyond such sat point, the magnetic material behaves like air. The B(H) curve thus has two parts, a nonlinear part below the sat point and linear part above the sat point,

$$B = J + \mu_o H \quad H \le H_{sat}$$
$$= B_s + \mu_o H \quad H > H_{sat} \qquad .... \quad ....(3)$$

III. Prior Art

Methods for extrapolation of measured B(H) to saturation have evolved over more than a century. Bozorth [1] traces many historical efforts, including the classic Frolich's hyperbolic model that is oft used by some manufacturers. Recently Umenei [16] and Kefalas [14] reviewed modern developments in the area. Ref. [14] [21] [11] attempt to fit a single-expression B(H) function to interpolate within the measured range and also to extrapolate outside the measured range. However, no single function could possibly replicate diverse mechanisms such as domain displacement, rotations, alignment and saturation that occur when the magnetic field intensity H varies over four to five decades. So approaches that use a single function for both interpolation and extrapolation of measured data are discounted.

Specifically, an earlier Exponential Law of Extrapolation (ELE) discussed in [11] [16] proposes an exponentially decaying function

$$J = B_s(1 - e^{-\beta H}).$$

But it calculates the saturation induction B_s solely from the last data point, so any noise in the last point can corrupt the calculated B_s. The Law of Approach to Saturation (LAS) outlined in [1] [16] [22] proposes a polynomial

$$J = B_s(1 - b/H^2).$$

This also calculates B_s from a single point alone. The Saturation Field Extrapolation (SFE) is similar to SLE but it adds one more point to extrapolation [16], so is inconsistent with physics of saturation. The Kaido's function

$$H = ae^{bB} + cB^n$$

does not obey the laws of saturation [21]; it also appears to be limited to 5000 A/m, which is far from saturation.

Most design software employ a procedure called Straight Line Extrapolation (SLE) [16] [14] [33]. SLE assumes that B(H) curve becomes a straight-line after the last measurement point. The slope of this straight-line varies with software. Some software packages assume that the slope of this line equals 1 (i.e., the material is assumed to saturate at the last measured point B_n). Others assume that the slope equals that derived from the last two points (i.e., the material is assumed to never saturate). Some others add a new point and use resulting new slope between the last point and the new point. Most major manufacturers use in-house software to find out the limits of overfluxing, and some attempt to extrapolate other functions such as ν(B), H(B), ν(B^2), $\mu_r(H^2)$ where ν = $1/\mu_r$ denotes reluctivity. For example, [10] [14] [53] extrapolate over the reluctivity function ν(B^2). None of these extrapolation methods include the saturation induction B_s as input data in the extrapolation process. This results in a B(H) curve that has no guarantee to saturate and deviates from actual B(H) curve at high fields, thereby potentially skewing results [16] [34] [51]. In view of these deficiencies, an ideal function that produces low error in extrapolation seems to have eluded the investigators so far. The proposed SEE extrapolation function described below attempts to fill this gap.

IV. Simultaneous Extrapolation to Saturation

The three functions B(H), J(H), D(H) shown in Fig. 1 simultaneously characterize the extrapolation to saturation. The proposed simultaneous extrapolation methods (termed SEE and SPE) fit these three functions simultaneously. The functions are chosen to meet the previously stated requirements for extrapolation to saturation. Both methods also utilize a known B_s, thereby circumventing the need to calculate it from the measured data that rarely predicts it accurately. We describe herein these two extrapolation methods.

The *Simultaneous Exponential Extrapolation* (SEE) uses a ferric flux density function J(H) that employs an exponential function which reaches asymptotically a known saturation induction B_s at which the magnetic material saturates. Thus, SEE forces the extrapolation process to automatically follow the laws of saturation. The three extrapolation functions used by SEE are

$$J(H) = B_s(1 - ae^{-bH})$$
$$B(H) = B_s(1 - ae^{-bH}) + \mu_0 H \quad \ldots \quad \ldots \quad (4)$$
$$D(H) = 1 + \frac{B_s}{\mu_o} abe^{-bH}$$

The two unknown coefficients a, b are determined from the measured data set. The coefficient a is dimensionless while the coefficient b has [m/A] units.

The *Simultaneous Polynomial Extrapolation* (SPE) uses a ferric flux density function J(H) that employs inverse polynomials, which reaches asymptotically a known saturation B_s at which the magnetic material saturates. The three extrapolation functions used by SPE are

$$J = B_s(1-\frac{c}{H^d})$$

$$B = B_s(1-\frac{c}{H^d}) + \mu_0 H \quad \cdots \quad \cdots \quad (5)$$

$$D = 1 + \frac{B_s}{\mu_o}\frac{cd}{H^{d+1}}$$

As in SEE, the two unknown coefficients c and d (both dimensionless) are determined from the measured data.

A. Estimating the Coefficients

We calculate the extrapolation coefficients a,b, c, d using following constraints:

a) They fit all usable data points of B(H) and D(H) simultaneously minimize the error ε.

b) The error ε is sum of absolute error fractions at all usable points of both B(H) and D(H) curves. (One can also use the least squares error metric without affecting the results)

$$\varepsilon = \sum \left| \frac{D_i - D(H_i)}{D_i} \right| + \left| \frac{B_i - B(H_i)}{B_i} \right| \quad \cdots \quad \cdots (6)$$

c) All functions may pass through chosen knot points (see section 6). The last point B_n, D_n or sat point B_{sat} are typical knot points. Using the sat point as a knot point essentially converts the extrapolation problem into an interpolation problem.

d) The D_{sat} calculated by the D(H) extrapolation function must be slightly more than one.

e) The J_{sat} calculated by the J(H) extrapolation function must be slightly smaller than the known saturation induction B_s.

B. Estimating Saturation Induction Bs

Generally, it is preferable to use a measured value of saturation induction B_s in eq. (4) or (5). For a specific steel, one can measure B_s from one of several standards, viz. ASTM A341, A773, or A596. A341 uses DC permeameters, A773 uses ring specimens while A596 uses a yoked circuit [47]. If no measured B_s is available, one can estimate it from resistivity ρ (μΩ cm) as follows. It is well known that B_s reduces almost linearly with percentage of Silicon, as per several references, e.g., [1] [3] [4] [5] [46]. Similarly, the resistivity ρ is known to increase almost linearly with percentage of Silicon, as per plots in [3] [4] [5]. Fig. 2 replots these data on a common silicon percentage scale.

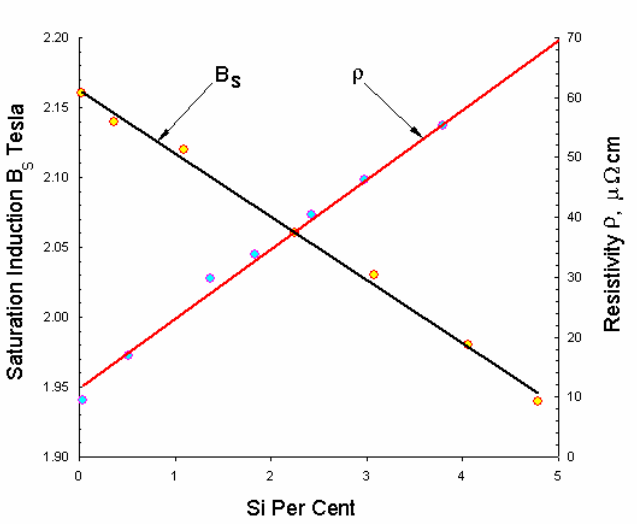

Fig. 2 Silicon percentage controls both the Saturation Induction B_S and resistivity ρ almost linearly. So one can use the Saturation Induction (calculated from a known resistivity ρ) to extrapolate the measured data so it follows saturation laws.

A simple straight line-fit of this data then yields following empirical formulas for B_s vs. silicon percent (s) and resistivity ρ with silicon percent (s):

$$B_s = 2.1668 - 0.043s \quad \cdots \quad \cdots \quad (7)$$

$$\rho = 10 + 11.54s$$

As a result, B_s can be estimated for any electrical steel using the following empirical formula when its resistivity ρ is known:

$$B_s = 2.2041 - 0.003726\rho \quad \cdots \quad (8)$$

For example for M-4, a steel manufacturer supplied ρ = 48μΩcm and stated that its magnetic induction is B_s = 2.035T [45]. For this resistivity, the empirical formula (8) yields an estimated value of B_s = 2.025T. Thus, the estimated value of 2.025 T for saturation induction deviates from the measured value of 2.035 T by only 0.5% , which is within an experimental scatter band.

C. Examples

a) A manufacturer's data for M250-35A electrical steel at 50 Hz ends at a last point of B_n = 1.8T [50]. The slope at this last measured point is D_n =18, indicating that it an order of magnitude away from saturation (D = 1). This steel has resistivity of 55 μΩ cm per the manufacturer. So from eq. (8) its saturation induction is B_s = 2T. Further, prior tests have indicated that the sat point H_{sat} is 100,000 A/m [15]. So, we use this data to generate the SEE and SPE extrapolation functions in accordance with procedures laid in section IV. Figs. 3, 4, 5 compare respectively the J(H), B(H) and D(H) extrapolation functions from SEE, SPE and other prior procedures. Dots in these figures denote the measured data points. The SEE extrapolation curve is shown in green color. The color scheme used to identify the prior extrapolation

functions are as follows: ELE (dashed), SPE (brown), LAS (pink) and SLE (red). A recent extrapolation method devised in [53], is shown in blue. Fig. 3 shows that the method in [53] does not saturate the material.

SEE extrapolation is accurate. The SEE yielded an extrapolation error of ε =14% and fitted data with coefficients a=0.345, b= 9.98E-5. Fig. 3 for J yields J_{sat} = 1.999T - which is close to the saturation induction B_s = 2 T. Fig. 5 for the slope yields D_{sat} = 1.002 - which is 0.2% above the saturation slope of 1. Both confirm that SEE ensures that the chosen sat point is close to saturation. Fig. 5 also shows that the slope D for SEE transitions smoothly from last data point. It also shows that the slope D of other functions changes abruptly at the last data point. It is hence clear that the proposed SEE method is more accurate than other procedures.

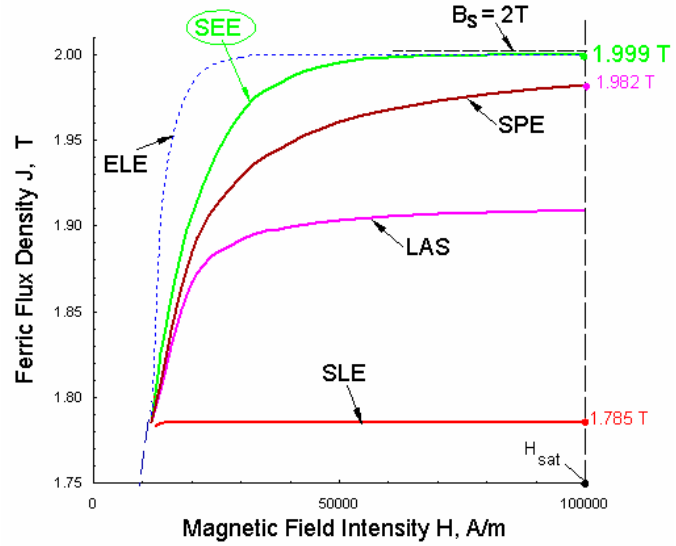

Fig. 3 J(H) curves of M250-35A steel per SEE vs. prior procedures. It shows that the SLE extrapolation procedure - used by some simulation software - causes large errors.

SPE extrapolation is less accurate. The SPE yielded a large error of ε = 505%, and fitted c= 6015 and d = 1.167. This large error indicates that SPE does not fit the measured data well. Fig. 3 shows J_{sat} = 1.982 T while Fig. 5 shows its slope D_{sat} = 1.16 - 16% above the saturation slope of one. Both indicate that SPE extrapolation does not saturate the material at the sat point. Fig. 4 also shows its B(H) curve differs significantly from that of SEE. Thus, SPE is no match to SEE in accuracy.

LAS extrapolation produces large error. The LAS resulted in an unusually high error of ε = 1300% and fitted coefficient b=8.97E6. This large error indicates poor fit of measured data to saturation. Fig. 3 shows J_{sat} =1.91 T vs. B_s = 2 T or 4.5% error in saturation point. Fig. 5 shows D_{sat} = 1.03 or 3% above the saturation slope. B(H) curve for LAS in Fig. 4 differs significantly from that of SEE curve. All these factors signify that the LAS extrapolation is relatively poor.

ELE yielded incorrect B_s. The ELE produced an error ε = 438% and fitted the coefficient β = 0.00027. ELE also estimated B_s as 1.864 T vs. actual B_s of 2T - a 7% error in saturation. This large error is caused by the use of only one point to calculate B_s. Fig. 5 also shows that ELE that the material saturates at ~ 30,000 A/m (instead of 100,000 A/m). All these factors indicate that ELE extrapolation is not as accurate as SEE.

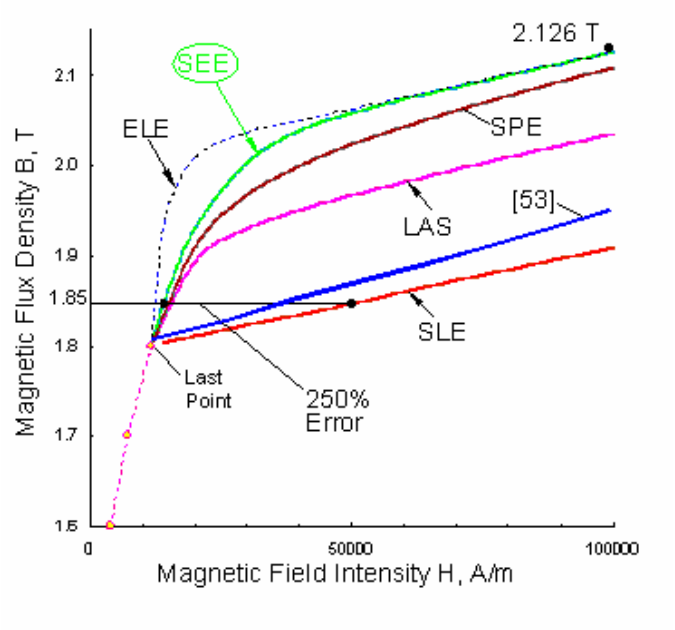

Fig. 4 B(H) Curves per SEE vs. prior procedures. To attain same flux density, the SLE - used by some simulation software - demands significantly larger field intensity.

SLE produces largest error. The curves for SLE shown here reflect the results from a leading finite element magnetic simulation software. It can be seen that the ferric flux density J(H) curves predicted by SLE differs drastically from that of SEE. This indicates that the SLE extrapolation does not saturate the material. The D(H) curve for SLE extrapolation shows the material saturating at 15000 A/m (very early instead of 100,000 A/m). Fig. 4 also shows SLE greatly distorts the B(H) curve. Fig. 4 shows that, to attain 1.85T, SEE requires 14,200 A/m. In contrast, the SLE extrapolation demands 50,000 A/m. Thus, SLE demands 250% more current than SEE to achieve same flux density. Thus, SLE extrapolation can overestimate the current needed to attain a given flux density.

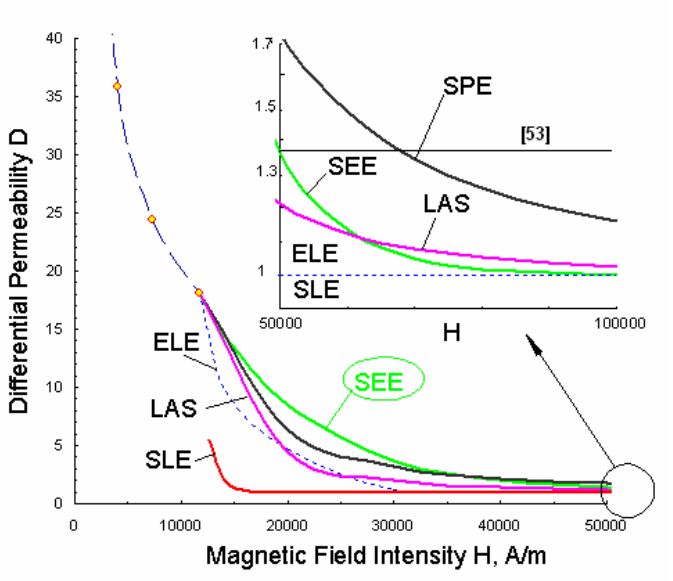

Fig. 5 D(H) Curves per SEE vs. prior procedures. Even though all extrapolations eventually reach the saturation slope of one, the SLE produces unacceptably large discontinuity at the last measured point.

b) Fig. 6 presents last few test data points for 1010 steel; it shows that the slope at the last data point of B_n =1.8T is D_n = 32 (an order of magnitude away from saturation). The sat point is known to be B_{sat} = 2.324T at H_{sat} = 200,000 A/m [42] [43]. Eq. (1) then yields B_s = 2.07T. The SEE procedure outlined in section IV is used to estimate the B(H) (blue), J(H) (pink) and D(H) (red) curves. The SEE resulted in ferric flux density of J_{sat} = 2.069 T at 100,000 A/m, close to the B_s = 2.07T. In contrast, Fig. 6 shows that the SLE extrapolation greatly distorts the B(H) curve. For example, it shows that, at 100,000 A/m, the material attains flux density B of only 1.9T instead of 2.19T. Further, Fig. 6 shows that, in order to attain 1.84T, SEE requires 6,200 A/m while SLE demands 40,000 A/m. Thus, SLE overestimates the current required by 545 %.

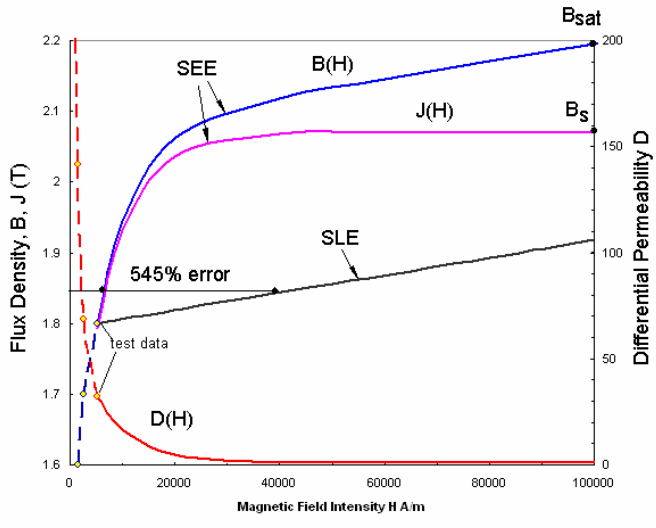

Fig. 6 B(H), J(H) and D(H) extrapolation curves for 1010 steel per SEE vs. that generated by an SLE procedure used by a leading simulation software. SLE demands 545% larger field intensity H to attain same flux density.

V. HIDDEN NOISE VS. NUMERICAL STABILITY

Interpolating functions that fit B(H) data can be grouped into two broad categories. In the first category, one attempted to fit a single-valued B(H) function over the entire magnetization data. Such historic attempts trace back to Rayleigh [1], Weiss and Langevin [1] [40] etc. (Similar efforts by Preisach [44] and Jiles-Atherton [41] etc. to fit a multi-valued B(H) function over all hysteresis loops are outside the scope of this paper). Recent investigators tried to fit hyperbolic tangent functions [40], [41] [24] [29], polynomials [6] [7] [9], exponentials [6] [10] [11] [36] [38], trigonometric [6], [11] - [14], [20] or combinations [21]. But a single interpolating function may not faithfully represent all phases of magnetization, such as reversible and irreversible domain wall movements, rotations and field alignments at atomic level and eventual saturation. It may also miss the initial and peak permeability, or may distort the μ_r(H), J(H) or D(H) curves [19]. A single function cannot interpolate exactly (with 0 % error) at all data points. In fact, there can be considerable error between the measured and interpolated values at some points. Because of these diverse deficiencies, fitting a single interpolating function over the entire measured data has gone out of fashion about twenty years ago.

Currently most software fit multiple interpolating functions to the measured B-H data, each being accurate over a smaller segment of data, each being continuous in first and second derivatives. Such multiple *spline functions* can interpolate exactly at the end points (called knots) of a smaller segment of data with 0 % error [35]. Examples used by magnetic field software include, but not limited to, cubic splines [8] [33] [37] , Hermite polynomials [34] or Bezier functions. While the spline functions offer relatively low error for interpolation, they often produce large errors when used to extrapolate beyond the measured range, so cannot be trusted for extrapolation to saturation.

For numerical stability and fast convergence the B(H) functions must be monotonic (i.e., continuous and increase monotonically) while its slope D(H) must be smooth (i.e., continuously increase monotonically, reach a single peak and continuously decrease monotonically, without any oscillations around the single peak). Around the single peak point (point of inflexion), the slope of the D(H) curve is positive on one side and negative on the other side. This single peak, representing the point of inflexion, is a theoretical point of instability.

The slope D(H) curve of measured data can sometimes show multiple peaks around this point of instability [35] [33], which reflect hidden noise. Such hidden noise, seen in the D(H) curve but not in the B(H) curve, is not removed by the interpolating functions. Multiple peaks around the point of instability confuse the iterative schemes used in the simulation software, leading to increased computational time or

instability.

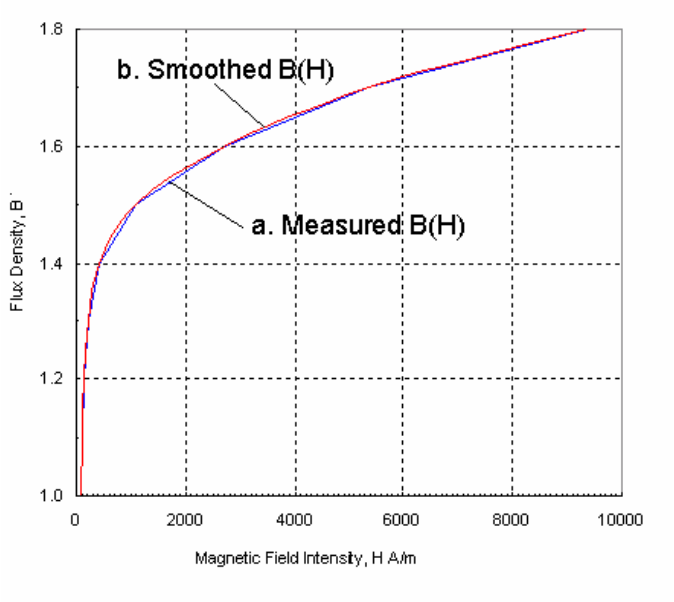

Fig. 7 (a) Measured B(H) curve (blue) plotted from manufacturer's data and (b) smoothed B(H) after removing the noise (red). Noise hidden in the manufacturer's data caused numerical instability and increased computational time.

Figs. 7 – 9 illustrate this process of removing the hidden noise in the measured data. Fig. 7(a) (blue) shows a measured manufacturer's B(H) curve for a 0.008-inch thick non-oriented electrical steel [50]. This measured B(H) curve is monotonic and continuous, but contains hidden noise. Fig. 7(b) (red) shows a smoothed B-H) curve, obtained after removing the hidden noise around the point of instability. Fig, 7 shows that the smoothed B(H) curve appear to be not much different from the measured B(H) curve. But inputting the smoothed B(H) curve into a commercial software resulted in a fast convergent solution while inputting the measured B(H) curve with hidden noise showed instability and slow convergence.

The hidden noise in the measured data is revealed in Fig. 8 which plots the slope D(H) of the magnetization curve around the point of instability. The measured D(H) curve shown in Fig. 8(a) is non-monotonic and has multiple peaks viz. the slope D oscillates around the point of instability. Such oscillations in the slope confuse the Newton-Raphson iteration schemes used by a software and hence cause numerical instability. Fig. 8b (red) plots a smoothed D(H) curve, obtained after removing such hidden noise. This curve shows only one peak and its usage resulted in numerically stable computation with fast convergence.

To ensure stability, thus one must remove the hidden noise (spurious peaks) and extract a smooth D(H) function that has only one peak and input that particular B(H) data into magnetic field software. This is done by plotting the D(H) curve in order to identify specific offending data points that cause the multiple peaks. The numerical values for H or B in such offending data points have to be modified until a smooth D(H) curve with a single peak is obtained. Only slight modification of the H values (usually at the first decimal place) is often sufficient to remove the hidden noise, viz., spurious multiple peaks, as seen in Fig. 8(b). We demonstrate herein that such smoothed B(H) data whose D(H) curve is smoothed, viz., has a single peak, greatly improves the numerical stability.

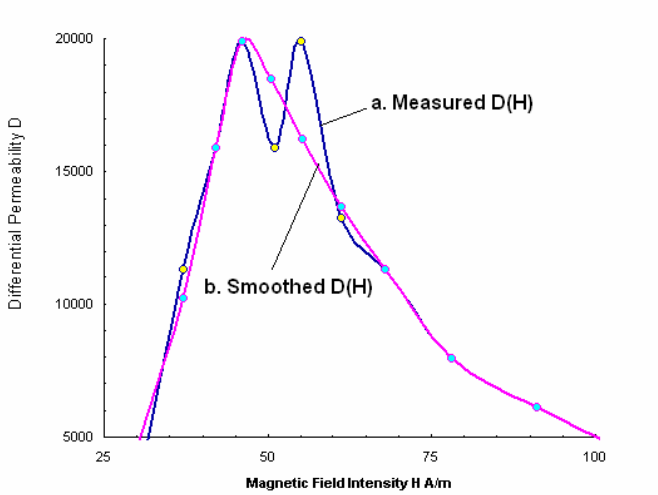

Fig. 8 (a) The measured D(H) curve (blue) plotted from manufacturer's data shows multiple peaks around the point of instability. This confuses the iterative algorithms used in commercial software and results in slow convergence. (b) The smoothed D(H) curve (pink), plotted after removing the hidden noise, shows a single peak. Its usage resulted in fast convergence.

To investigate the effect of hidden noise in the measured data on numerical stability, we simulated a three-phase induction motor (rated 1kW at 1400 rpm, driven by 230-volt supply) under transient (startup plus load-on), no-load and full load conditions. The outer diameter of the stator is 140 mm, its inner diameter is 80 mm, the stack length is 57mm; it has 36 slots while the rotor has 28 bars. A MotorAnalysis tool, written in Matlab [49] is used for assessing the impact of hidden noise on convergence. It is first used with the manufacturer's measured B(H) data and next with the smoothed B(H) data, obtained by the procedure described above. An integration step of 0.1 ms and a convergence tolerance of 10^{-4} are used in the simulation.

Table 1 summarizes the convergence information for both cases. The data is averaged over 5000 integration steps. Values in the parenthesis correspond to those obtained when manufacturer's measured B(H) data is used. This table indicates that smoothing the manufacturer's B(H) data reduces the computational time by 26%, 24% and 30% for transient, no-load and full load conditions respectively. Using smoothed data always resulted in a fast convergent solution. From this analysis, one can conclude that one should remove any noise hidden in the measured or manufacturer's B(H) data before inputting it into magnetic field software.

Table 1. Convergence of smoothed B(H) data (manufacturer's data in brackets)

Parameter	Transient	No-load	Full load
Number of iterations	4.5 (6.5)	4.1(5.8)	7.5 (5)
Computation time [s]	49.9 (67)	45.9 (60.7)	53 (75.5)
Convergence error %	0 (78)	0 (4)	0 (147)

Fig. 9 shows the number of Newton iterations vs. integration steps. Fig. 9(a) shows how the smoothed B(H) data causes stable convergence of solution in all conditions. Fig. 9(b) shows that the manufacturer B(H) data greatly increases computation time and causes instability or non-convergence. It also shows red circles that mark points where solution failed to converge. Comparing both simulations confirms that removing the hidden noise in the measured B(H) curve results in stable convergence.

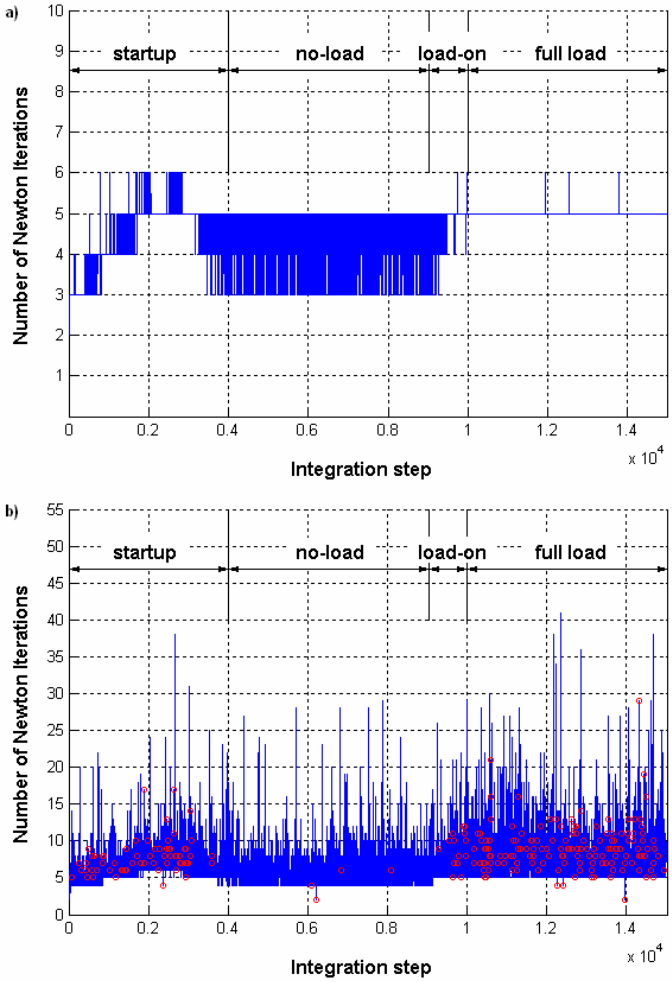

Fig. 9 Number of iterations vs. integration steps for an induction motor. a) Inputting smoothed B(H) data into magnetic field software shows fast convergence. b) Inputting the manufacturer's measured B(H)data caused significant numerical instability and failed to converge. Red circles mark points of non-convergence.

VI. Conclusions

Torque-dense electric machines in severe operating conditions can show overfluxed regions that carry substantially large magnetic fields, and they could severely damage the machine. Often such damage-prone regions are in the deep saturation regime, where the measured B-H data is rarely available. Accurate mapping of the overfluxed regions therefore requires carefully engineered extrapolation to saturation. This paper proposed two procedures for such extrapolation. Both incorporate the physics of saturation in the process. The illustrative examples presented herein indicate that the Simultaneous Exponential Extrapolation (SEE) procedure offers greater accuracy than other procedures developed so far.

This paper has also shown that the measured or manufacturer data can contain hidden noise that can cause numerical instability. The B(H) curve does not reveal this hidden noise. But its slope, viz D(H) curve can reveal the hidden noise by way of multiple peaks around the point of instability. We proposed a graphical procedure to attain a smoothed B(H) data, with the hidden noise removed. Usage of such smoothed B(H) data is shown to increase the computational speed.

In summary, this paper proposed a SEE procedure for extrapolation of the measured B-H data to saturation. This can assist in mapping overfluxed regions, thereby limiting their adverse impact on electric machines. It also presented a graphical procedure to remove any hidden noise in the measured data. Inputting such smoothed data into a field software increases the computational speed. Magnetic material databases that use both procedures will help control the adverse impact of overfluxed regions on the performance of electric machines.

References

[1] R. M. Bozorth, *Ferromagnetism*, New York, IEEE Press, 1993, pp. 7, 476-487.
[2] H. C. Roters, *Electromagnetic Devices*, John Wiley & Sons, 1941, pp. 23-24.
[3] P. Beckley, *Electrical Steel for Rotating Machines*, Stevenage, UK: IET, 2002, p. 24.
[4] J. K. Stanley, *Electrical and Magnetic Properties of Metals*, Metals Park, OH: American Society of Metals, 1963, p. 284.
[5] F. Fiorillo and I. D. Mayergoyz, *Characterization and Measurement of Magnetic Materials*, Amsterdam: Elsevier B.V, 2004, p.39.
[6] F. C. Trutt, E. A. Erdelyi and R. E. Hopkins, "Representation of the magnetization characteristics of DC machines for computer use," *IEEE Trans. Power Engg*, Vol. PAS-87, No. 3, Mar. 1958, pp. 665-669.
[7] Anonymous [2013, July] Normal Magnetization Curve Fit Formulas. [Online] Available: http://www.mag-inc.com
[8] P. Silvester and R. Gupta, "Effective computational models for anisotropic soft B-H curves," *IEEE Trans. Magn.*, Vol. 27, No. 5, Sept. 1991, pp. 3804-3807.
[9] Anonymous [2013, July] Characteristics of Mur (B) of Common Soft Magnetic Materials. [Online] Available: http://www.maplesoft.com/documentation_center/online_manuals/modelica/Modelica_Magnetic_FluxTubes_Material_SoftMagnetic.html
[10] J. R. Bauer, "Simple equations for the magnetization and reluctivity curves of steel," *IEEE Trans. Magn.*, Vol. 11, No. 1, 1975, p 81.

[11] M. Jesenik, A. Hamler, P. Kitak and M. Trlep, "Parameters for expressing analytical magnetization curve obtained using a generic algorithm," *Compumag 2013*, Budapest, July 2013.
[12] I. Meszaros, "Magnetization curve modeling of soft magnetic alloys," *J. of Physics Conf. Series*, Vol. 268, No. 1, 2011, pp.1-6.
[13] I. Meszaros, "Complex Magnetic Characterization of Iron-Silicon Transformer Sheets," *J. Elec. Engg.*, Vol. 57, No. 8/9, 2006, pp.151-154.
[14] T. D. Kefalas and A.G. Kladas, "Analysis of transformers working under heavily saturated conditions in grid-connected renewable energy systems, " *IEEE Trans. Ind. Electron*., Vol. 59, No. 5, May 2012, pp. 2342-2350.
[15] Anonymous [2013, Sept] Magnetic Property Curves. [Online] Available: http://www.steel-n.com/esales/general/us/catalog/electrical/plate6.html
[16] A. E. Umenei, Y. Melikhov and D. C. Jiles, "Models for extrapolation of magnetization data on magnetic cores to high fields," *IEEE Trans. Magn*., vol. 47, No. 12, Dec. 2011, pp. 4706-4711.
[17] K. W. Chen and T. Glad, "Estimation of the primary current in a saturated transformer," *Proc. 30th IEEE Conf. on Decision Control*, Vol. 3, Dec. 1991, pp. 2363-2365.
[18] Z. Wlodarski, "Analytical description of magnetization curves," *Physica B Condensed Matter*, vol. 373, No. 2, 2006, pp 323-327.
[19] M. Jaafar, V. Markovski and M. Elleuch, "Modeling of differential permeability and the initial magnetization curve of ferromagnetic materials," *IEEE Int. Conf on Industrial Technology*, vol. 1, 2004, pp. 460-465
[20] M. T. Abuelman'atti, "Modeling of magnetization curves for computer-aided design," *IEEE Trans. Magn*, vol. 29, no. 2, Mar. 1993, pp. 1235 - 1239.
[21] C. Kaido, "Modeling of Magnetization Curves in Non-oriented Electrical Steel Sheets," *Elec. Engg. Japan*, vol. 180, No. 3, 2012, pp. 1-8.
[22] V. A. Ignatchenko, R. S, Iskhakov and G. V. Popov, "Law of Approach of the Magnetization to saturation in amorphous ferromagnets," *Soviet Physics JETP*, vol. 66, No. 5, May 1982, pp. 878-888.
[23] S. Zurek, F. Al-Naemi, A. J. Moses and P. Marketos, "Anomalous B-H behavior of electrical steels at very low flux density," *Journal of . Magnetism and Magnetic Materials*, Vol. 320, No. 20, Oct. 2008, pp. 2521-2525.
[24] D. Lederer, H. Igarashi, A. Kost, and T. Hanma. "On the parameter identification and application of the Jiles-Atherton hysteresis model for numerical modelling of measured characteristics," *IEEE Trans. Magn*, Vol. 35, No. 3, May 1999, pp. 2011-2014.
[25] Skyworks [2013, April] Test for Saturation Magnetization, Application Note No. 663. [Online] Available: http://www.trans-techinc.com/documents/Test_for_Saturation_Magnetization_202838A.pdf
[26] G. G. Orenchak [2013, May] Specify saturation properties of ferrite cores to prevent field failure. [Online] Available: http://www.elnamagnetics.com/wp-content/uploads/library/TSC-Ferrite-International/Specify_Saturation_Properties_of_Ferrite_Cores_to_Prevent_Field_Failure.pdf
[27] R. Becker, G. Martinez and A. V. D. Weth, "Improvement of magnetic field calculations by extrapolation," *Nuclear Instruments and Methods in Physics Research Section A*, vol. 519, No. 2, Feb. 2004, pp. 49-52.
[28] R. L. Sanford, "A determination of the magnetic saturation induction of iron at room temperature," *J. Res. Nat. Bur Stand*, vol. 26, No. 1, Jan. 1941, pp 1-12.
[29] J. Rivas, J. M. Zamarro, E. Martin and C. Pereira, "Simple approximation for Magnetization curves and hysteresis loops," *IEEE Trans. Magn.*, vol. 17, No. 4, July 1981, pp. 1498-2502.
[30] R. F. Smith, J. O. Nichols, "Analysis of a deep bar induction motor and compressor load during start-up," *IEEE Trans. on Power Apparatus and Sys*., vol. PAS-97, No. 5, Sep. 1978, pp. 1696-1705.
[31] G. K. M. Khan, G. W. Buckley, R. B. Bennett, N. Brooks, "An integrated approach for the calculation of losses and temperatures in the end-region of large turbine generators," *IEEE Trans. On Energy Conversion*, vol. 5, No. 1, Mar. 1990, pp. 183-194.
[32] G. Klempner and I. Kerszenbaum, *Operation and Maintenance of large turbogenerators*, John Wiley & Sons: Hoboken, NJ, July 2004, p. 46.
[33] K. Hameyer and R. Belmans, *Numerical modeling and design of electric machines*, WIT Press, Boston, pp. 90-94.
[34] D. A. Lowther and P. P. Silvester, *Computer aided design in magnetics*, Springer Berlin Heidelberg, 1986, chapter 2, pp. 13-36.
[35] C. Pechstein and B. Juttler, "Monotonicity-preserving interproximation of B-H curves," *J. Computational and Applied Mathematics*. vol. 196, No. 1, Nov. 2006, pp. 45-57.
[36] J. H. Hwang and W. Lord, " Exponential series for B/H Curve modeling," *Proc. I.E.E.*, vol. 123, No. 6, 1976.
[37] M. H. Nagrial, and S. J. Ashraf, "B/H curve approximation for computer aided designs of electromagnetic devices," *Elec. Machines & Power Systems*, vol. 6, No. 3, 1981, pp. 207-213.
[38] M. K. El-Sherbiny, "Representation of the magnetization characteristic by a sum of exponentials," *IEEE Transactions on Magnetics*, vol. Mag-9, No. 1, Mar. 1973, pp. 60-61.
[39] L Janicke, A. Kost, et al., "Numerical modeling for anisotropic magnetic media including saturation effects," *IEEE Trans. Magn*, Vol. 33, No 2, 1997, pp. 1788-1791.
[40] P. Langevin, "Magnetism and electron theory," *Annals. Chem. Physics*, vol. 5, 1905, pp. 70-127.
[41] D. C. Jiles and D. L. Aetherton, "Theory of ferromagnetic hysteresis," *J. Magn. Magn. Mat.*, Vol. 61, 1986, pp. 48-60.
[42] *Metals Handbook*, 8th Ed., American Society of Metals, 1966, p. 792.
[43] Anonymous [2013, May] Finite Element Method Magnetics. [Online] Available: http://www.femm.info/wiki/HomePage
[44] F. Preisach, Uber die magnetische nachwirkung, *Zeitschrift fur Physik*, vol. 94, 1935, pp. 277-302.
[45] *Grain-Oriented Electrical Steel Technical Data Sheet*, Allegheny Technologies Inc, Pittsburgh, PA
[46] A. Goldman, *Handbook of modern ferromagnetic materials*, Springer: Boston, MA, 1999, p.117.
[47] S. Tumanski, *Handbook of magnetic measurements*, CRC Press Series in Sensors, Boca Raton, FL, June 2011, p. 9.
[48] ASTM A343/2008, *Standard test method for alternating-current properties of materials at power frequencies using wattmeter-ammeter-voltmeter method and 25-cm Epstein test frame*, ASTM, West Conshohocken, PA, 1993.
[49] V. Kuptsov, [2014, May] FEA-based electrical machine design application, [Online] Available: http://motoranalysis.com
[50] Cogent [2014, Feb] Non-Oriented Electrical Steel, [Online] Available: http://www.sura.se/Sura/hp_main.nsf/startupFrameset?ReadForm
[51] M. V. Zagirnayak, Yu. A. Branspitz, "Improvement of account the nonlinearity of iron magnetic characteristics in electromagnetic computation," *J. Kremenchuk State Polytechnic University, Electromechanics and Automation Section*, vol. 53, No. 6, 2008. [Online] Available: http://www.kdu.edu.ua/statti/2008-6-1/7.pdf
[52] S. Meier [2014, April] Influence of the B-H Curve on the convergence of the finite element solution [Online] Available: https://www.emetor.com/blog/post/influence-b-h-curve-convergence-finite-element-solution/
[53] A. M. Knight and D. G. Dorrell, "Improving the torque prediction of saturated automotive drive machines by accurate representation of saturated B/H curves," *IEEE Trans. Magn.*, vol. 48, No. 11, Nov. 2012, pp. 4630-4633.
[54] Z. Azar, Z. Q. Zhu, G. Ombach, "Influence of Electric Loading and Magnetic Saturation on Cogging Torque, Back-EMF and Torque Ripple of PM Machines", *IEEE Trans. Magn.*, vol. 48, No. 10, Oct. 2012, 2650-2658.
[55] J. M. Miller, A. R. Gale, P. J. McCleer, F. Leonardi, J. H. Lang, "Starter-alternator for hybrid electric vehicle: comparison of induction and variable reluctance machines and drives," *33rd IEEE Industry Application Conference*, vol. 1, Oct. 1998, pp. 513-523.
[56] K. C. Kim, "Analysis on Correlation Between Cogging Torque and Torque Ripple by Considering Magnetic Saturation" , IEEE Trans. Magnetics, vol. 49, No. 5, May 2013, 2417-2420.
[57] Q. C. Qu, "Precise magnetic properties measurement on electrical sheet steel sheets under deep saturation", *IEEE Trans. Magn*., vol. 20, No. 5, Sept. 1984, 1717-1719.
[58] C. A. Charalambous, R. Zhang, Z. D. Wang, "Simulating thermal conditions around core bolts when transformer is experiencing ferroresonance, " *Int. Conf. Power Systems Transients*, Delft, Netherland, June 14-17, 2011.
[59] C. A. Charalambous, Z. D. Wang, P. Jarman, J. P. Sturgess, "Time-domain finite element technique for quantifying the effect of sustained ferroresonance on power transformer core bolts," IET Electr. Power Appl., Vol. 8, No. 6, July 2014, pp.221-231.

Dantam K. Rao was born in 1944 in India. He received his Ph.D from Indian Institute of Technology, Kharagpur, India, in 1971. He served as a Professor there until 1984. He conducted research in electro-mechanical interactions at Wright Patterson Laboratory, Dayton, OH in 1984-87. He served as Project Manager of magnetic and superconducting bearings in Mechanical Technology Inc., Albany, NY from 1987. He was president of a small business developing torque-dense electric motors since 1995. He was senior electromagnetic engineer at General Electric Co., from which position he retired in 2010. Currently he is Technical Director at MagWeb USA, NY. His research interests include electromagnetics, heat transfer, high voltage insulation systems, deep brain stimulation and transcranial magnetic stimulation.

Vladimir V. Kuptsov was born in Russian Federation in 1984. He received the Engineering Degree in industrial electronics from Magnitogorsk State Technical University, Magnitogorsk, Russian Federation in 2007 and Ph.D. degree in electrical engineering from Magnitogorsk State Technical University, Magnitogorsk, in 2010.

Since 2007 he has been an engineer in Magnitogorsk Iron and Steel Works where he is currently engaged in R&D group of Technical Diagnostics Department. His research interests include electric machine modeling, finite element analysis, signal processing and fault diagnostics.